with the top in place and the bottom cut out.

The mounted tooth was removed from the capsule and sawed or ground on an industrial belt sander so that a longitudinal section of the tooth was exposed. This exposed section was then polished by hand on 600 alumina grit paper and examined under a binocular microscope with reflected light at a magnification of $\times$ 40 to $\times$ 150 power. We were often able to enhance the visual contrast by wetting the specimen with ethanol.

Sectioning of encapsulated teeth has produced analyzable sections from archeological contexts where decalcification has failed or has succeeded on only a small proportion of teeth. Initial experiments with teeth from the Turner Farm were largely successful. It appears that the individuals examined were killed during the winter and possibly early spring (Figs. 1 and 2). This pattern, if confirmed by future tests, supplements other seasonal data and raises the interesting possibility that the site was occupied during much of the year, especially during the late Archaic period. Initial success with specimens from the Turner Farm led us to test teeth from other North American sites (Fig. 2).

Although incremental layers as observed in solid sections may lack the high contrast of those from decalcified thin sections, they are usually analyzable if present. In some instances, where initial observations were inconclusive, repolishing produced clearer results (repolishing is essentially analogous to the preparation of multiple thin sections from decalcified teeth).

Thus, solid sectioning appears to give results roughly comparable to decalcification but with less risk of destruction. For the novice, however, the lowered contrast may make it more difficult to analyze the section relative to the case for decalcified and stained thin sections. Surprisingly, the times required for the preparation of solid and decalcified sections is roughly equal: about 15 minutes per tooth, disregarding unattended time of plastic hardening or decalcification. However, decalcification is a relatively delicate procedure requiring sophisticated equipment whereas grinding solid sections is a "low technology" approach which might even be attempted as a short-range analytical technique in field laboratories.

We caution that the periodicity and seasonal significance of incremental growth layers is clearly established for only a relatively small number of species, primarily those from temperate and arctic North America. Therefore, we urge caution in extrapolating patterns observed in modern teeth to unstudied species.

BRUCE J. BOURQUE, KENNETH MORRIS
Maine State Museum, Augusta 04330
ARTHUR SPIESS
Peabody Museum, Harvard University, Cambridge, Massachusetts 021388

References

1. R. W. Casteel, *Am. Antiq.* **37** (No. 3), 404 (1972); A. C. Ziegler, *Inference from Prehistoric Faunal Remains* (Module in Anthropology No. 43, Addison-Wesley, Reading, Mass., 1973).
2. A. Spiess, *Arctic* **29** (No. 1), 53 (1976).
3. B. J. Bourque, *Arctic Anthropol.* **12** (No. 2), 35 (1975); *Man Northeast No. 11* (1976), p. 21.
4. B. Peyer, in *Comparative Odontology*, R. Zangerl, Ed. (Univ. of Chicago Press, Chicago, 1968), p. 13.

4 October 1977; revised 11 November 1977

Images of Io's Sodium Cloud

Abstract. *The first direct images of Io's sodium cloud are reported and analyzed. The observed cloud extends for more than 10^5 kilometers along Io's orbit and is a somewhat "banana-shaped" partial toroid. More sodium atoms precede Io than follow it. A model based on the escape of sodium from a specific localized area on Io provides a reasonable fit to the observed intensity distribution whereas isotropic escape does not.*

Io, the innermost of Jupiter's Galilean satellites, has long been known for its unusual properties. Io has the highest reflectance of any object in the solar system and governs the bursts of decametric radiation from the jovian magnetosphere. Spectral reflectance data suggest that it has evaporite minerals or "salts" on its surface (*1*). In 1973 Brown discovered that sodium atomic line emissions were emanating from Io (*2*). The sodium is distributed throughout an immense volume about Io and fluoresces in its resonant D lines in proportion to the available sunlight (*3*). The source of the sodium is believed to be Io's surface material. Sodium could be released by the sputtering action of magnetospheric proton and ion bombardment, and much of it would have sufficient velocity to escape from the satellite (*4*). Neutral sodium atoms are removed from the cloud chiefly by electron impact ionization whereupon emission in the characteristic D lines is no longer possible (*5*).

In order to understand the processes governing the production and loss of sodium in the cloud, we must know the spatial distribution of sodium about Io. In this report we describe two images that we have obtained of Io's sodium cloud (Figs. 1 and 2) and report the first results of the study of these images. A more detailed analysis of these and other images will appear elsewhere (*6*). The two images were obtained with the coudé spectrograph at the 61-cm (24-inch) telescope at Table Mountain Observatory. Instead of the usual spectrograph entrance slit, we substituted a thin plate of glass upon which a small spot of aluminum was deposited. During an exposure the image of Io was guided near the center of this occulting element, thus excluding the solar continuum reflected by Io from the spectrograph. Atomic line emission from the surrounding cloud, however, was permitted to enter the spectrograph. This radiation was dispersed by the grating into distinct components corresponding to each of the sodium lines. At the focus of the spectrograph the "slit" or object plane was imaged, and two images corresponding to the D_1 and D_2 emission lines were seen. Since the portion of the cloud closest to Io was blocked by the occulting disk, the shadow of the disk is present in the cloud images. All data were recorded with a silicon imaging photometer system (SIPS) with a silicon intensifier tube (RCA 4804) (*7*). In our observations the spectral smearing of the image due to the finite width of the emission lines is comparable in amplitude to the uncertainties introduced into the images by astronomical "seeing." Thus the effect is not significant for the present data set.

The cloud images demonstrate that the sodium is distributed asymmetrically about Io. The sodium emission was most intense in the west at the time these data were taken; both images show considerably less sodium emission to the east and to the north and south. The cloud in Fig. 1 is seen to extend westward from Io some 50 arc seconds or about 1.9×10^5 km. This extension is less in Fig. 2 because of foreshortening resulting from a different viewing angle. These two images, considered together, indicate that the sodium extends along Io's orbit as suggested by Carlson *et al.* (*5*). The observed geometry is compatible with a partial toroid shaped somewhat like a banana. It is not consistent with the high velocity radial streaming model which

0036-8075/78/0203-0531$00.50/0

would tend to give a spherical distribution (8, 9). Furthermore, as one can see from a comparison of the low eastern intensity in Figs. 1 and 2, Io itself must reside in the rear portion of the cloud relative to the common direction of motion of the satellite and its sodium cloud about Jupiter. This idea is consistent with the suggestion by Bergstralh *et al.* (10) that more sodium precedes Io in its orbit than follows it.

In both images the sodium intensity distributions grade smoothly into the background noise at the level of a few kilorayleighs (11). Thus the cloud probably extends to greater distances but is below our threshold of detection. Data obtained with high-speed spectrographs have established the existence of the sodium cloud at least halfway along Io's orbital path (that is, on the other side of Jupiter) where the intensities are much less than those in the present images (12).

These images provide a new means to test models of the sodium production and loss mechanisms. Theoretical models of Io's interaction with the jovian magnetosphere (13) lead one to suggest that sputtering may occur over localized regions of Io's surface (4). In Fig. 1 we compare the observed intensity distribution in the image with distributions pre-

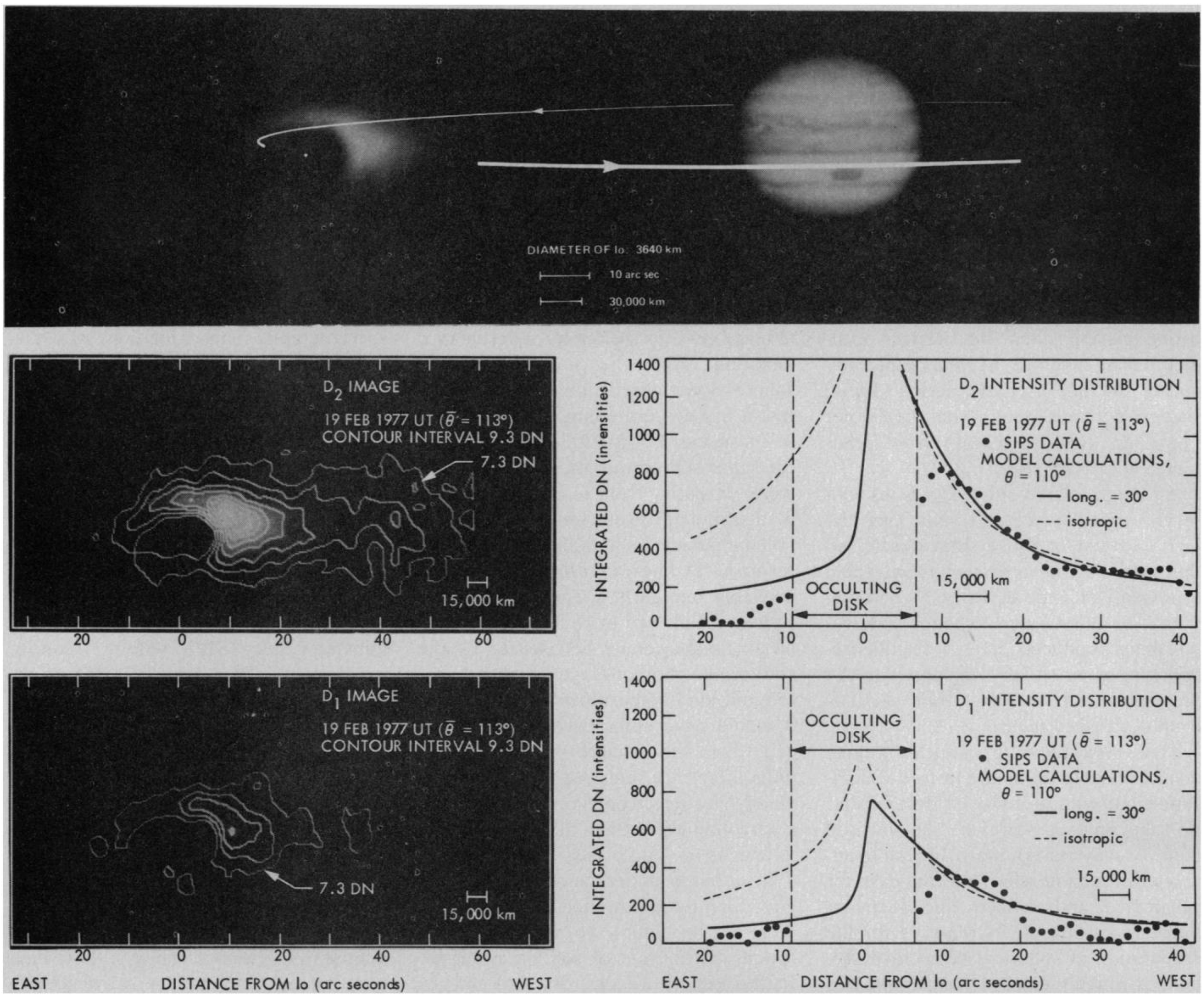

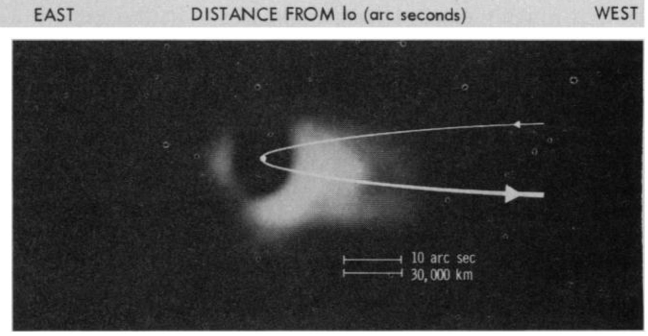

Fig. 1 (above). Image of Io's sodium cloud (D_1 + D_2) taken on 19 February 1977 U.T. at Table Mountain Observatory (top). A picture of Jupiter and a drawing of the orbital geometry have been added to orient the reader. Exposure time was 3 hours. The dark area within the sodium cloud is the shadow of the occulting disk which was used to keep reflected sunlight from Io itself out of the spectrograph. The small white dot indicates the position and size of Io. Individual D_2 and D_1 images are shown (lower left) with superimposed intensity contours. The 7.3 DN contour corresponds to about 2 to 4 kR (11). The rest wavelengths are, respectively, 5890 and 5896 Å; $\bar{\theta}$ is the average orbital phase angle for the exposure. The integrated east-west intensity distributions are shown at the lower right. The observed distributions rule out the isotropic model but are compatible with the hemispheric sputtering model centered at 30° longitude on Io's equator. Fig. 2 (below right). Image of Io's extended sodium cloud (D_1 + D_2) taken on 3 December 1976 U.T. at Table Mountain Observatory. Drawings of the oribtal geometry and Io's disk are included for perspective. Io's orbital radius is 421,600 km. Exposure time was 3.5 hours. The occulting disk used for this exposure was less elliptical than that used for Fig. 1. Comparison with Fig. 1 (which shows a different amount of foreshortening) demonstrates that the cloud is elongated and that more sodium precedes Io than follows it.

dicted by two of our sputtering models. The two model curves were obtained by assuming (i) isotropic sodium ejection from Io and (ii) sodium escape from a single hemisphere only (centered on Io's equator at 30° longitude; 0° longitude faces Jupiter, and 90° is the leading point in the orbit). An initial velocity distribution characteristic of sputtering was used (*14*). Atmospheric effects were neglected. We traced the subsequent velocities and positions, using a three-body forward numerical calculation. The assumed $1/e$ ionization time was 10^5 seconds (*5*). The computed density distribution was then projected in perspective seen from Earth (*15*). For the purpose of comparison, we have summed the data columns to obtain an integrated east-to-west profile (Fig. 1).

The general agreement between the hemispheric model and observation is good. There are, of course, no useful data at the position of the occulting disk. Furthermore, "seeing" introduces a spurious drop in the intensity for a few arc seconds beyond the disk's edge. There is a further drop caused by the wavelength smear due to the changing Doppler shift of the cloud during our 3.5-hour exposure. These effects are evident, for example, out to 3 arc seconds west of the disk's edge (a reasonable distance considering both "seeing" and the difficulties of guiding during long exposures). Since the projection of the cloud changes with time, the orbital motion of the cloud also contributes a small amount of spatial smear to the image. Although the model fits less well in the eastern portion of the cloud, the signal level here is low. The intensity levels are thus sensitive to any error in the dark current subtraction, in the interpolation scheme used to reduce the effects of background-scattered light, and in the effective location of Io relative to the occulting disk.

Both the image data reported here and independent spectral-line profile data (*14*) show that nonisotropic models are necessary (*16*). The asymmetries may be due to (i) the distribution of sodium across Io's surface, (ii) the sputtering process, or (iii) the jovian magnetospheric plasma, including its interactions with Io. Earth-based telescopic observations of Io's surface reveal albedo and color variations of continental size. These color differences may be due to compositional variations of presently unknown magnitude. Thus, it is conceivable that there are places on Io where the sodium concentration is relatively low. Second, the sputtering process itself may not operate uniformly over Io's surface. One need only consider the two different ionospheres observed from one side of Io to the other on the Pioneer 10 mission (*17*) and the various plasma sheath models developed in attempts to understand Io's interaction with the magnetosphere (*13*). Both these lines of evidence indicate that large spatial variations in the charged particle and electromagnetic field environment are to be expected. Since sputtering is dominated by charged particle impacts, the sputtering rate can be greatly enhanced or retarded by localized electromagnetic fields. Finally, the magnetospheric plasma interaction with Io is not symmetrical. The plasma overtakes Io with a relative velocity of 56 km sec^{-1}. This plasma flows past Io and its flux tube, causing fluctuations in the plasma density. These fluctuations may lead in turn to significant variations in the rate at which neutral sodium is ionized, depending upon its location with respect to Io and the magnetosphere. Although we cannot rule out any of these processes, we find that our hemispheric source model gives an adequate fit to the available data.

The direct images presented here are the first obtained of Io's sodium cloud. They provide a clearer picture of the cloud's geometry than earlier images and have aided in the refinement of theoretical models. In the future, imaging promises to be an important tool in the understanding of Io's surface composition and interaction with the jovian magnetosphere and of processes operative in the cloud.

DENNIS L. MATSON
BRUCE A. GOLDBERG
TORRENCE V. JOHNSON
ROBERT W. CARLSON

Space Sciences Division,
Jet Propulsion Laboratory,
Pasadena, California 91103

References and Notes

1. F. P. Fanale, T. V. Johnson, D. L. Matson, *Science* **186**, 922 (1974); in *Planetary Satellites*, J. Burnes, Ed. (Univ. of Arizona Press, Tucson, 1977), p. 379. It is likely that sodium is a relatively abundant element in Io's surface material. Fanale *et al.* have analyzed the available data on Io and have concluded that the satellite's surface is composed of certain types of sodium-rich evaporite minerals and elemental sulfur. This type of composition follows as a consequence of Jupiter's luminosity history, the opacity, the temperature and composition of the circumjovian nebula from which the satellites accreted, and the present intense radiation environment. The depositional environment could also have produced evaporite deposits relatively rich in potassium, an element that has also been detected in the cloud [L. Trafton, *Nature (London)* **258**, 690 (1975)].
2. R. A. Brown, in *Exploration of the Planetary System, Proceedings of I.A.U. Copernicus Symposium 4 (International Astronomical Union Symposium No. 65)*, A. Woszczyk and C. Iwaniszewska, Eds. (Reidel, Dordrecht, 1974), p. 527. This paper on the discovery of sodium atomic line emissions from Io was first presented in 1973. Additional background material may be found in the review by R. A. Brown and Y. L. Yung, in *Jupiter*, T. Gehrels, Ed. (Univ. of Arizona Press, Tucson, 1976), p. 1102.
3. The extended nature of the sodium emission from Io was first recognized by Trafton *et al.* (*8*). Trafton *et al.* and Matson *et al.* (*4*) realized simultaneously that resonant scattering was the mechanism responsible for the emission. The demonstration that the emission bore the time-dependent intensity signature characteristic of resonant scattering (that is, Io orbits Jupiter and "sees" Fraunhofer lines periodically Doppler-shifted; as a result different amounts of sunlight are available for scattering) was made by Bergstralh *et al.* (*10*).
4. D. L. Matson, T. V. Johnson, F. P. Fanale, *Astrophys. J. (Lett.)* **192**, L43 (1974).
5. R. W. Carlson, D. L. Matson, T. V. Johnson, *Geophys. Res. Lett.* **2** 469 (1975).
6. B. A. Goldberg, D. L. Matson, T. V. Johnson, R. W. Carlson, in preparation.
7. The SIPS frame format was 256 by 256 pixels with 8-bit digitization. The data were processed at the Image Processing Laboratory of the Jet Propulsion Laboratory according to the following procedure: (i) subtraction of the nominal dark current, (ii) calibration of the individual pixel response with the use of a "flat field" frame obtained by means of a tungsten lamp, (iii) geometry correction (rotation), (iv) spatial filtering, (v) linear interpolation to estimate and remove residual dispersed continuum radiation which inadvertently fell into the spectrograph, (vi) contrast enhancement, (vii) intensity contouring and for the D_1 and D_2 image of Fig. 1 only, and (viii) superposition and summation of the D_1 and D_2 images. Most of these techniques have been used previously and extensively in the processing of spacecraft images. Their detailed application will be discussed elsewhere (*6*). Geometric distortion is better than 10 percent.
8. L. M. Trafton, T. D. Parkinson, W. Macy, Jr., *Astrophys. J. (Lett.)* **190**, L85 (1974).
9. L. Trafton, *ibid.* **202**, L107 (1975).
10. J. T. Bergstralh, D. L. Matson, T. V. Johnson, *ibid.* **195**, L131 (1975).
11. One rayleigh (R) is the apparent emission rate of 10^6 photon cm^{-2} sec^{-1} for an isotropic (that is, 4π steradian) emitter. The area unit refers to an atmospheric column [D. M. Hunten, F. E. Roach, J. W. Chamberlain, *J. Atmos. Terr. Phys.* **8**, 345 (1956); J. W. Chamberlain, *Physics of the Aurora and Airglow* (Academic Press, New York, 1961), p. 569]. We have obtained the calibration of the emission contours for our instrumental sensitivity, using Io's continuum level. We estimate the uncertainty of this procedure as systematically plus or minus a few kilorayleighs for the 7.3 digital number (DN) contour. The relative levels are precise to within several DN. The overall level of emission observed is consistent with data reported by other observers [for example, W. Macy, Jr., and L. Trafton, *Astrophys. J.* **200**, 510 (1975); L. Trafton and W. Macy, Jr., *Astrophys. J. (Lett.)* **202**, L155 (1975)].
12. Y. Mekler and A. Eviatar, *Astrophys. J. (Lett.)* **193**, L151 (1974); P. A. Wehinger, S. Wyckoff, A. Frohlich, *Icarus* **27**, 425 (1976).
13. For example, see D. A. Gurnett, *Astrophys. J.* **175**, 525 (1972); S. D. Shawhan, *J. Geophys. Res.* **81**, 3373 (1976).
14. R. W. Carlson, D. L. Matson, T. V. Johnson, J. T. Bergstralh, *Astrophys. J.*, in press.
15. For additional details, see (*5*) and (*14*). The excitation function for sodium D lines does not change rapidly at an orbital phase angle of 110° [see, for example, Bergstralh *et al.* (*10*), figure 2], and thus the density distribution can be compared directly with observation.
16. Currently the line profile data (*14*) are better fitted by a model with the hemisphere of sputtering centered at a longitude of 90°, compared to a longitude of 30° used here. We regard this difference as one indication of the level of uncertainty in the current modeling.
17. A. Kliore, D. L. Cain, G. Fjeldbo, B. L. Seidel, S. I. Rasool, *Science* **183**, 323 (1974).
18. We thank J. Colin Mahoney and James Young for important contributions which made these images possible. We gratefully acknowledge the assistance of Joel Mosher and J. Andreas Howell in the reduction of the data at the Image Processing Laboratory. One of us (D.L.M.) acknowledges helpful conversations with Larry M. Trafton (University of Texas, Austin) during an earlier and unsuccessful effort to obtain images of Io's sodium cloud. This work represents one phase of the research carried out at the Jet Propulsion Laboratory under NASA contract NAS 7-100.

2 August 1977; revised 11 October 1977